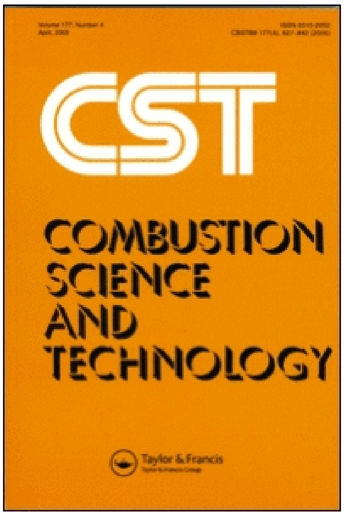

Combustion Science and Technology
Publication details, including instructions for authors and subscription information:
http://www.informaworld.com/smpp/title~content=t713456315

Studies on the Outwardly and Inwardly Propagating Spherical Flames with Radiative Loss

Zheng Chen [a]; Xiaolong Gou [b]; Yiguang Ju [c]
[a] SKLTCS, Department of Mechanics and Aerospace Engineering, College of Engineering, Peking University, Beijing, China [b] School of Power Engineering, Chongqing University, Chongqing, China [c] Department of Mechanical and Aerospace Engineering, Princeton University, Princeton, New Jersey, USA

Online publication date: 03 February 2010

To cite this Article Chen, Zheng, Gou, Xiaolong and Ju, Yiguang(2010) 'Studies on the Outwardly and Inwardly Propagating Spherical Flames with Radiative Loss', Combustion Science and Technology, 182: 2, 124 — 142
To link to this Article: DOI: 10.1080/00102200903299850
URL: http://dx.doi.org/10.1080/00102200903299850

Combust. Sci. and Tech., 182: 124–142, 2010

ISSN: 0010-2202 print/1563-521X online
DOI: 10.1080/00102200903299850

STUDIES ON THE OUTWARDLY AND INWARDLY PROPAGATING SPHERICAL FLAMES WITH RADIATIVE LOSS

Zheng Chen,[1] Xiaolong Gou,[2] and Yiguang Ju[3]
[1]*SKLTCS, Department of Mechanics and Aerospace Engineering, College of Engineering, Peking University, Beijing, China*
[2]*School of Power Engineering, Chongqing University, Chongqing, China*
[3]*Department of Mechanical and Aerospace Engineering, Princeton University, Princeton, New Jersey, USA*

Outwardly and inwardly propagating spherical flames (OPF and IPF) with radiative loss are studied analytically and numerically. Emphasis is placed on investigating the effects of radiation on flame propagating speed, Markstein length, and flame extinction, as well as on examining whether the reactant can be completely consumed via an IPF. A general correlation between flame propagating speed and flame radius for OPF and IPF of large flame radii is derived and utilized to study the effects of radiative loss and Lewis number on flame propagation and extinction. A correlation for Markstein length at different Lewis numbers and radiative loss is also presented. It is shown that the Markstein length is strongly affected by radiative loss as well as Lewis number, and that only for mixtures not close to their flammability limits and without CO_2 dilution is the effect of radiation on the Markstein length measured from expanding spherical flames negligible. Furthermore, the theoretical results are validated by numerical simulations. It is found that when radiative loss is considered, there exists unconsumed reactant after the extinction of IPF for mixture with Lewis number less than unity.

Keywords: Extinction; Markstein length; Propagating spherical flame; Radiative loss

INTRODUCTION

It is well known that radiative heat transfer is a dominant mechanism for near limit flames. Indeed, the flammability limit is determined by radiative loss for unstretched premixed planar flames (Buckmaster, 1976; Spalding, 1957). However, for stretched flames, the flammability limit can be changed by the combined effects of thermal radiation and flame stretch, which were studied by using the counterflow flames (Buckmaster, 1997; Ju et al., 1997; Sohrab & Law, 1984). These studies showed that the flammability limit of stretched flames below a critical Lewis number can be lower than that of unstretched flames. However, unlike the counterflow

Received 21 March 2009; revised 6 June 2009; accepted 31 August 2009.
Address correspondence to Zheng Chen, State Key Laboratory of Turbulence and Complex Systems (SKLTCS), College of Engineering, Peking University, Beijing 100871, China. E-mail: cz@pku.edu.cn

flames, practical flames—such as the laminar propagating spherical flames used in microgravity experiments and the flamelets in turbulent flames—are not only stretched but also curved. To include the curvature effect, the tubular flames (Ishizuka, 1993; Ju et al., 1999; Mosbacher et al., 2003) and outwardly propagating spherical flames (Bechtold et al., 2005; Chen & Ju, 2007; Ronney & Sivashinsky, 1989) were utilized to study the combined effects of flame radiation, stretch, and curvature on premixed flames. It was shown that the interaction of flame curvature and radiative loss greatly affects the flame propagation and extinction.

The counterflow flames, outwardly propagating spherical flames (OPF), and tubular flames all have positive stretch rate. In order to study the effect of negative flame stretch rate, the inwardly propagating spherical flames (IPF) can be utilized. The quenching of IPF was studied theoretically and numerically (Flaherty et al., 1985; Frankel & Sivashinsky, 1983, 1984; Sivashinsky, 1974; Sun & Law, 1998). The quenching was found to take place at non-zero velocity of the flame front for mixtures with Lewis number less than unity due to the negative stretch rate of IPF. For mixtures with Lewis number larger than unity, it was shown that extinction also occurs for IPF due to depletion of the upstream mixture (Sun & Law, 1998). However, radiative loss was not considered in all of the above studies on IPF. As a result, how radiation affects the propagation and extinction of IPF remains unknown. The first objective of this study is hence to reveal the effects of radiation on propagation and extinction of OPF and IPF.

Recently, the method utilizing propagating spherical flames in a closed chamber becomes one of the most favorable methods for measuring laminar flame speed and Markstein length (see Chen et al., 2009a, 2009b; Huang et al., 2006; and references therein). Radiation transfer is inevitable in practical experiments, and the effect of radiation on flame speed measurements has been investigated in previous studies (Buckmaster & Lee, 1992; Chen et al., 2007; Taylor, 1991). However, there is no study on how the Markstein length is affected by radiation. Therefore, the second objective of this study is to investigate the effects of radiation on Markstein length using OPF and IPF.

Finally, we note that flame extinction caused by radiation is one of the most important problems on engine performance for ultra-lean combustion utilized in high-efficiency low-emission engines such as the HCCI. The extinction of IPF could be a source of unburned hydrocarbon and constitute a loss in the combustion efficiency in internal combustion engines (Sun & Law, 1998). When radiation was not considered, numerical simulations of IPF (Flaherty et al., 1985; Sun & Law, 1998) showed that extinction is caused by the depletion of lean reactant, and there is no unconsumed reactant. However, it is not clear whether this also happens to IPF with radiative loss. The third objective of this study is therefore to examine whether the reactant can be completely consumed via IPF with radiative loss.

Based on the objectives discussed above, the OPF and IPF with radiative loss will be investigated analytically and numerically in the following. First, the mathematical model is presented. Second, theoretical analysis of OPF and IPF is conducted to investigate the effects of radiative loss on flame propagation, flame extinction, and Markstein length. Finally, numerical simulations of OPF and IPF are performed to validate the theoretical results and to examine whether there is unconsumed reactant for IPF with radiative loss.

MATHEMATICAL MODEL

Figure 1 shows the schematic diagrams of OPF and IPF investigated in this study. By assuming constant thermal properties, the conservation equations for energy and fuel mass fraction are given as

$$\tilde{\rho}\widetilde{C}_p \frac{\partial \widetilde{T}}{\partial \tilde{t}} = \frac{1}{\tilde{r}^2}\frac{\partial}{\partial \tilde{r}}\left(\tilde{r}^2\tilde{\lambda}\frac{\partial \widetilde{T}}{\partial \tilde{r}}\right) - \widetilde{H} + \tilde{q}\tilde{\omega} \tag{1}$$

$$\tilde{\rho}\frac{\partial \widetilde{Y}}{\partial \tilde{t}} = \frac{1}{\tilde{r}^2}\frac{\partial}{\partial \tilde{r}}\left(\tilde{r}^2\tilde{\rho}\widetilde{D}\frac{\partial \widetilde{Y}}{\partial \tilde{r}}\right) - \tilde{\omega} \tag{2}$$

where $\tilde{t}, \tilde{r}, \tilde{\rho}, \widetilde{T}$, and $\widetilde{Y}$ are time, radial coordinate, density, temperature, and fuel mass fraction, respectively. $\tilde{q}$ is the chemical heat release per unit mass of fuel, $\widetilde{C}_P$ the specific heat capacity at constant pressure, $\tilde{\lambda}$ the thermal conductivity, and $\widetilde{D}$ the fuel mass diffusivity. To further simplify the problem in theoretical analysis, we also adopt the commonly used constant density model (Frankel & Sivashinsky, 1984; Joulin & Clavin, 1979; Williams, 1985) so that the convection flux is absent. The reaction rate for a one-step irreversible reaction is $\tilde{\omega} = \tilde{\rho}\widetilde{A}\widetilde{Y}\exp(\widetilde{E}/\widetilde{R}^0\widetilde{T})$, in which $\widetilde{A}$ is the pre-factor of Arrhenius law, $\widetilde{E}$ the activation energy, and $\widetilde{R}^0$ the universal gas constant. The volumetric radiative loss $\widetilde{H}$ is estimated by using the optically thin model, $\widetilde{H} = 4\tilde{\sigma}\widetilde{K}_p(\widetilde{T}^4 - \widetilde{T}_\infty^4)$, where $\tilde{\sigma}$ is the Stefan-Boltzmann constant and $\widetilde{K}_p$ denotes the Planck mean absorption coefficient of the mixture.

By using the adiabatic planar flame speed, $\widetilde{S}_L^0$, and the flame thickness, $\tilde{\delta}_f^0 = \tilde{\lambda}/\tilde{\rho}\widetilde{C}_p\widetilde{S}_L^0$, the velocity, length, time, temperature, and fuel (lean) mass fraction can be normalized as

$$\tilde{u} = \frac{\tilde{u}}{\widetilde{S}_L^0}, \quad r = \frac{\tilde{r}}{\tilde{\delta}_f^0}, \quad t = \frac{\tilde{t}}{\tilde{\delta}_f^0/\widetilde{S}_L^0}, \quad T = \frac{\widetilde{T} - \widetilde{T}}{\widetilde{T}_{ad} - \widetilde{T}_\infty}, \quad Y = \frac{\widetilde{Y}}{\widetilde{Y}_\infty} \tag{3}$$

where $\widetilde{T}_\infty$ and $\widetilde{Y}_\infty$ denote the temperature and fuel mass fraction in the fresh mixture, respectively, and $\widetilde{T}_{ad} = \widetilde{T}_\infty + \widetilde{Y}_\infty\tilde{q}/\widetilde{C}_p$ is the adiabatic flame temperature. By further

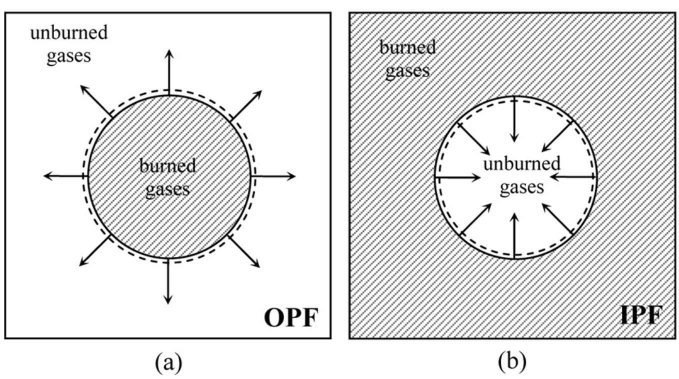

Figure 1 The schematic diagrams of (a) the outwardly propagating spherical flame (OPF) and (b) the inwardly propagating spherical flame (IPF) (Frankel & Sivashinsky, 1983).

attaching the coordinate to the moving flame front, $R = R(t)$, the non-dimensional equations take the following form in the new coordinate ($\tau = t$, $\xi = r - R(t)$)

$$\frac{\partial T}{\partial \tau} - \frac{dR}{dt}\frac{\partial T}{\partial \xi} = \frac{1}{(\xi + R)^2}\frac{\partial}{\partial \xi}\left[(\xi + R)^2\frac{\partial T}{\partial \xi}\right] - H + \omega \tag{4}$$

$$\frac{\partial Y}{\partial \tau} - \frac{dR}{dt}\frac{\partial Y}{\partial \xi} = \frac{Le^{-1}}{(\xi + R)^2}\frac{\partial}{\partial \xi}\left[(\xi + R)^2\frac{\partial Y}{\partial \xi}\right] - \omega \tag{5}$$

where $Le = \tilde{\lambda}/\tilde{\rho}\widetilde{C}_p\widetilde{D}$ is the Lewis number and dR/dt the flame front propagating speed. The radiative loss and chemical reaction rate are normalized, respectively, as

$$H = \frac{\widetilde{H}\tilde{\delta}_f^0}{\tilde{\rho}\widetilde{C}_p\widetilde{S}_L^0(\widetilde{T}_{ad} - \widetilde{T}_\infty)}, \omega = \frac{\tilde{\omega}\tilde{\delta}_f^0}{\tilde{\rho}\widetilde{S}_L^0\widetilde{Y}_\infty} \tag{6}$$

In this study, the thermo-diffusion structure of the flame is assumed to be quasi-planar ($R \gg \xi$) (Frankel & Sivashinsky, 1983, 1984), and in the attached coordinate moving with flame front, the flame can be considered as in quasi-steady state ($\partial/\partial\tau = 0$). This quasi-steady assumption has been widely used in previous studies (Chen & Ju, 2007; Frankel & Sivashinsky, 1983, 1984) and validated by transient numerical simulation (Chen & Ju, 2007). As a result, the governing equations are simplified to

$$-\left(\frac{dR}{dt} + \frac{2}{R}\right)\frac{dT}{d\xi} = \frac{d^2T}{d\xi^2} - h \cdot T + \omega \tag{7}$$

$$-\left(Le\frac{dR}{dt} + \frac{2}{R}\right)\frac{dY}{d\xi} = \frac{d^2Y}{d\xi^2} - Le \cdot \omega \tag{8}$$

where the radiative loss term, H, is approximated by a linear function of normalized temperature as $H = h \cdot T$ for the convenience of the algebraic manipulation. h is the radiative loss constant ($h \ll 1$), which takes the following form:

$$h = \frac{4\tilde{\delta}\widetilde{K}_p\tilde{\delta}_f^0(\widetilde{T}^4 - \widetilde{T}_\infty^4)}{\tilde{\rho}\widetilde{C}_p\widetilde{S}_L^0(\widetilde{T} - \widetilde{T}_\infty)} \approx \frac{4\tilde{\sigma}\widetilde{K}_p\tilde{\lambda}}{(\tilde{\rho}\widetilde{C}_p\widetilde{S}_L^0)}\widetilde{T}_{ad}^3 \tag{9}$$

It is noted that the radiative loss constant involves the radiation intensity and the fuel concentration. For any mixture composition, a decrease of fuel concentration (decrease of flame speed) means an increase of h. For methane-air flames, the heat loss constant h is in the range of 0.001 to 0.05 (Chen & Ju, 2008). In the limit of large activation energy, chemical reaction occurs only within a very thin zone of high temperature, and the reaction rate can be replaced by a Delta function with jump conditions used at the flame front (Joulin & Clavin, 1979; Law, 2006):

$$\omega = \exp\left[\frac{Z}{2}\frac{T_f - 1}{\sigma + (1 - \sigma)T_f}\right] \cdot \delta(\xi) \tag{10}$$

where $Z = \widetilde{E}(1-\sigma)/\widetilde{R}^0\widetilde{T}_{ad}$ is the Zel'dovich number and $\sigma = \widetilde{T}_\infty/\widetilde{T}_{ad}$ the thermal expansion ratio. Integrating Eqs. (7) and (8) around the flame interface, the following jump relations can be readily obtained:

$$\left.\frac{dT}{d\xi}\right|_{\xi^-} - \left.\frac{dT}{d\xi}\right|_{\xi^+} = \frac{1}{Le}\left(\left.\frac{dY}{d\xi}\right|_{\xi^+} - \left.\frac{dY}{d\xi}\right|_{\xi^-}\right) = \exp\left[\frac{Z}{2}\frac{T_f-1}{\sigma+(1-\sigma)T_f}\right] \tag{11}$$

By defining the flame as the location where fuel concentration goes to zero, the boundary conditions for temperature and fuel mass fraction can be given as

$$\xi = -\infty, \quad dT/d\xi = 0, \quad dY/d\xi = 0 \tag{12}$$

$$\xi = 0, \quad T = T_f, \quad Y = 0 \tag{13}$$

$$\xi = \infty, \quad dT/d\xi = 0, \quad dY/d\xi = 0 \tag{14}$$

THEORETICAL ANALYSIS

Asymptotic Solutions

Equations (7) and (8) with boundary conditions given by Eqs. (12)–(14) can be solved analytically, and an exact solution of temperature and fuel mass fraction distribution is presented below. For fuel lean case, the fuel mass fraction in burned gas region is zero, and that in the unburned gas region is obtained by solving Eq. (8) with boundary conditions given by Eqs. (13) and (14). For OPF, we have

$$Y(\xi) = \begin{cases} 0 & for\ \xi \le 0 \\ 1-\exp\left[-\left(Le\frac{dR}{dt}+\frac{2}{R}\right)\right)\xi\right] & for\ \xi \le 0 \end{cases} \tag{15}$$

while for IPF, we have

$$Y(\xi) = \begin{cases} 1-\exp\left[-\left(Le\frac{dR}{dt}+\frac{2}{R}\right)\right)\xi\right] & for\ \xi \le 0 \\ 0 & for\ \xi \le 0 \end{cases} \tag{16}$$

As to the temperature distribution, the analytical solution for both OPF and IPF is

$$T(\xi) = \begin{cases} T_f\exp[(-V+\sqrt{V^2+dh})\xi/2] & for\ \xi \le 0 \\ T_f\exp[(-V-\sqrt{V^2+4h})\xi/2] & for \xi \ge 0 \end{cases} \tag{17}$$

where $V = dR/dt + 2/R$. By using the jump relations given by Eq. (11), one obtains the following algebraic system of equations for flame propagating speed, $dR/dt = V\text{-}2/R$, flame radius, R, and flame temperature, Tf,

$$T_f\sqrt{V^2+4h} = \pm\left[V+\frac{2}{R}\left(\frac{1}{Le}-1\right)\right] = \exp\left[\frac{Z}{2}\frac{T_f-1}{\sigma+(1-\sigma)T_f}\right] \tag{18}$$

where + is for OPF and − is for IPF. After eliminating the flame temperature in Eq. (18) with $h \ll 1$ (Chen & Ju, 2008), we have

$$\left(\frac{dR}{dt}+\frac{2}{R}\right)^2 \ln\left[\left(\frac{dR}{dt}+\frac{2}{R}\right)^2\right] = (Z-2)\frac{2}{R}\left(\frac{1}{Le}-1\right)\left(\frac{dR}{dt}+\frac{2}{R}\right) - L \tag{19}$$

where $L = 2Zh$. Using the above relationship, the effects of radiative loss on OPF and IPF can be investigated by comparing the flame propagating speed, $U = |dR/\mathrm{dt}|$, at different flame radii, R, and radiative loss intensities, L. The preferential diffusion (thermal versus mass diffusion) effect can also be studied by changing the Lewis number, Le, in Eq. (19).

It is noted that the present simplified model under the assumption of large flame radius ($R \gg 1$) works for both OPF and IPF, while the detailed model (Chen & Ju, 2007) without this assumption only works for OPF (there is no counterpart theory for IPF). The detailed model—Eq. (14) in Chen and Ju (2007), which works for OPF for all flame radii range—is found to reduce to the present result, Eq. (19) for OPF, in the limit of $R \gg 1$. Figure 2 shows the flame propagating speed as a function of flame radius for OPF predicted by the present simplified model and the detailed model in Chen and Ju (2007). It is seen that the prediction from the simplified model agrees well with that from the detailed model at different Lewis numbers and radiative loss. Moreover, the present simplified model also recovers previous results in different limiting cases:

- without radiative loss ($L = 0$), Eq. (19) reduces to that of adiabatic propagating spherical flames studied in Frankel and Sivashinsky (1984);

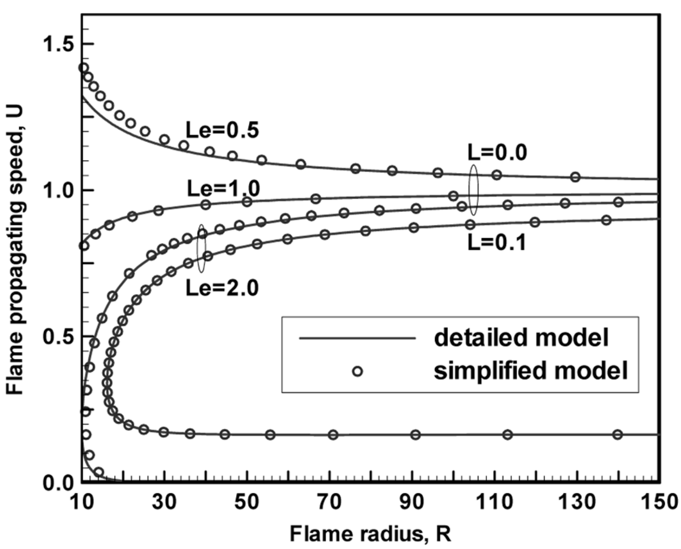

Figure 2 The flame propagating speed as a function of flame radius for OPF predicted by different models.

- by changing the curvature $2/R$ to $1/R$ in Eq. (19), the same result for non-adiabatic propagating cylindrical flames as that presented in Mitani (1980) is obtained; and
- in the limit of $R \to \infty$, Eq. (19) recovers the classical theory on flammability limit for planar flames (Joulin & Clavin, 1979):

$$(U^0)^2 \ln[(U^0)^2] = -L \tag{20}$$

where U^0 denotes the non-dimensional planar flame speed with radiative loss (normalized by the adiabatic planar flame speed). According to Eq. (20), the flammability limit for a planar flame is $L^* = 1/e \approx 0.37$ and $U^{0*} = \mathrm{e}^{-1/2} \approx 0.61$.

For both OPF and IPF, the Karlovitz number is defined as $K = (2/R)(dR/dt)$ (Clavin, 1985; Law, 2006). When it is small, $|K| \ll 1$, there is a linear relationship between the normalized flame speed, U, and K (Clavin, 1985):

$$U \approx U^0 - Ma \cdot K \tag{21}$$

where Ma is the Markstein number. Using Taylor expansion for Eq. (19) at small K, the linear relationship, Eq. (21), as well as the following expression for the Markstein number is obtained:

$$Ma = \frac{1}{U^0} - \frac{(Z/2 - 1)(Le^{-1} - 1)}{(U^0)[2\ln(U^0) + 1]} \tag{22}$$

According to Eqs. (20) and (22), it is seen that the Markstein number is affected not only by the Lewis number but also by the radiative loss. For adiabatic case ($L = 0$, $U^0 = 1$), the Markstein length (the subscript 0 means at zero radiative loss—i.e., adiabatic—while the superscript 0 means at zero stretch rate—i.e., unstretched) is

$$Ma_0 = Le^{-1} - (Z/2)(Le^{-1} - 1) \tag{23}$$

which is the same as that derived for adiabatic premixed counter flow flames (Law, 2006). In Law (2006), the following relationship is proposed for stretched premixed flames with small radiative loss ($L \ll 1$):

$$U \approx 1 - \left[\frac{1}{Le} - \frac{Z}{2}\left(\frac{1}{Le} - 1\right)\right]K - \frac{L}{2} \tag{24}$$

according to which the Markstein length is not affected by radiative loss and is a constant given by Eq. (23). This is not contradictory with the present result. The relationship given by Eq. (24) works only under small radiative loss, while the present results given by Eqs. (21) and (22) work well not only for small radiative loss but also for large radiative loss. As a result, the present theory works for a broader range of radiative loss, and hence the radiation effect on flame propagating speed as well as Markstein length at different Lewis numbers can be investigated using Eqs. (19) and (22).

Results and Discussion

Based on the theoretical results given by Eqs. (19) and (22), the effects of radiative loss and preferential diffusion (Lewis number) on flame propagation, flame extinction, and Markstein length are investigated. Figure 3 shows the normalized flame propagating speed as a function of flame radius for OPF and IPF with different radiative loss intensities and Lewis numbers. At a given Lewis number and radiative loss, there are two solutions of flame propagating speed for one specific flame radius: the fast stable one and the slow unstable one. Extinction occurs at the turning point where the fast branch meets the slow branch (Law, 2006). Figure 3 clearly shows that the *U*-*R* relation and flame extinction is strongly affected by the Lewis number as well as radiative loss. The *U*-*R* diagram of OPF and IPF shows totally opposite trends for $Le = 0.5$ and $Le = 2.0$. This is because, for a mixture with small/large Lewis number, the positive stretch rate (its magnitude continuously

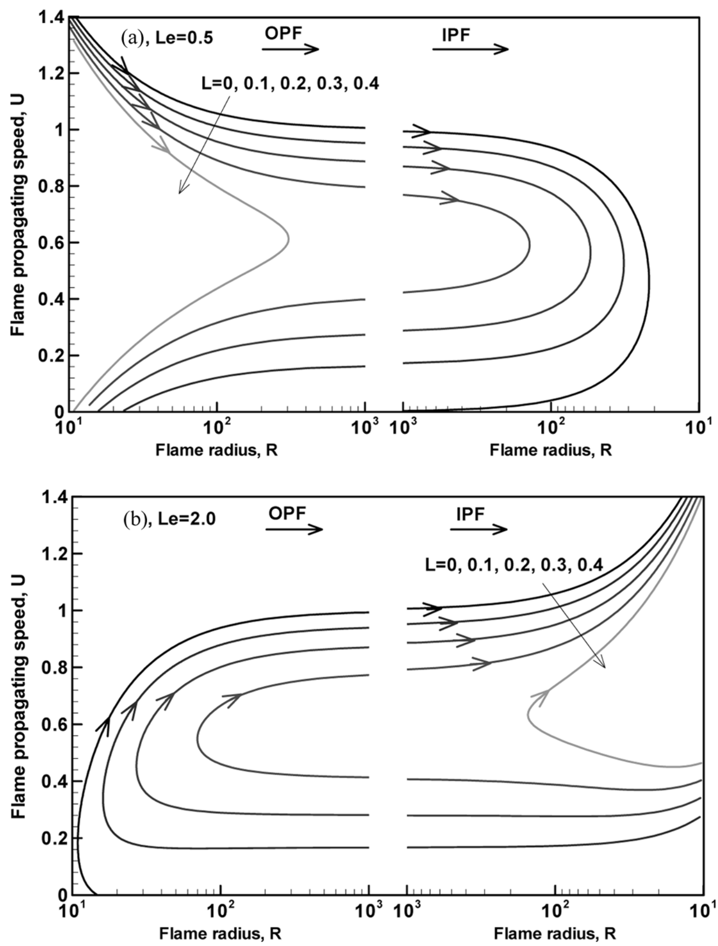

Figure 3 The flame propagating speed as a function of flame radius for OPF and IPF with different radiative loss: (a) $Le = 0.5$; (b) $Le = 2.0$.

decreases during propagation) of OPF strengthens/weakens the flame, and the negative stretch rate (its magnitude continuously increases during propagation) of IPF weakens/strengthens the flame (Clavin, 1985; Law, 2006). As a result, for $Le = 0.5$, the flame propagating speed (the fast stable branch) of both OPF and IPF decreases monotonically during propagation, while for $Le = 2.0$, it monotonically increases during propagation.

Moreover, Figure 3 shows that for $Le = 0.5$, extinction occurs for IPF even when the radiative loss is smaller than that corresponding to the planar flame flammability limit, $L^* = 1/e \approx 0.37$, while OPF still exists even for mixtures below the flammability limit, $L = 0.4 > 1/e = L^*$ (which is called self-extinguish flame, SEF). For OPF, the existence of SEF for mixture with a small Lewis number is because the flame stretch enhancement is greater than radiative loss when the flame radius is small (Ronney & Sivashinsky, 1989). For IPF, extinction is caused by the continuously increasing flame stretch effect, which weakens the flame during its propagation before the extinction point is reached. The opposite trend is found for $Le = 2.0$. Therefore, the flammability limit is changed by stretch rate coupled with preferential diffusion (Lewis number effect). This is further demonstrated by Figure 4. In Figure 4, the turning point on the solid curve ($R \to \infty$) corresponds to the flammability limit of planar flame, and only the upper fast branch is stable and thus physically realistic (Law, 2006). The dashed and dash-dotted lines represent solutions for propagating spherical flames at finite radii (thus finite stretch rate). The flammability region is shown to be either extended or reduced, depending on the value of the Lewis number and the sign of stretch rate: for mixture with small/large Lewis number, it is extended/reduced for positive stretch (OPF) and reduced/extended for negative stretch (IPF). The present results on flame stretch and Lewis number effects for OPF and IPF are consistent with those for OPF (Bechtold et al., 2005) and for counterflow flames (Law, 2006; Sohrab & Law, 1984).

To investigate the effects of radiation on the Markstein length, the normalized flame propagating speed as a function of stretch rate is shown in Figure 5. It is seen that the Markstein length (which is equal to the gradient in the U-K plot close to $K = 0$) is strongly affected by radiative loss: the gradient in the U-K plot increases with L for both OPF and IPF for $Le = 0.5$ and $Le = 2.0$. Quantitatively, the Markstein length can be evaluated for different Lewis numbers and radiative loss according to Eq. (22). Figure 6 shows the normalized Markstein number as a function of radiative loss for different Lewis numbers. It is seen that for small radiative loss, the Markstein length is close to that of the adiabatic flame, Ma_0. However, when the radiative loss is large, the Markstein length is strongly affected, especially when L is close to that corresponding to the flammability limit ($L^* = 1/e$). Furthermore, as can be observed from Figure 6, the change of the Markstein length due to radiative loss is also strongly affected by the Lewis number: the increase of Markstein length due to radiation for $Le = 1$ is shown to be smaller than that for $Le = 0.5$ and $Le = 2$, while the Markstein length decreases with radiative loss for $Le = 0.85$.

Figure 7 shows the normalized Markstein number as a function of Lewis number for different radiative loss. It is seen that the normalized Markstein number varies non-monotonically with the Lewis number and reaches infinity at $Le = 0.8$ due to the appearance of zero Ma_0 for $Z = 10$ (according to Eq. (23), Ma_0 is zero at $Le = 1\text{–}2/Z = 0.8$). With the increase of radiative loss, the magnitude of the Markstein number

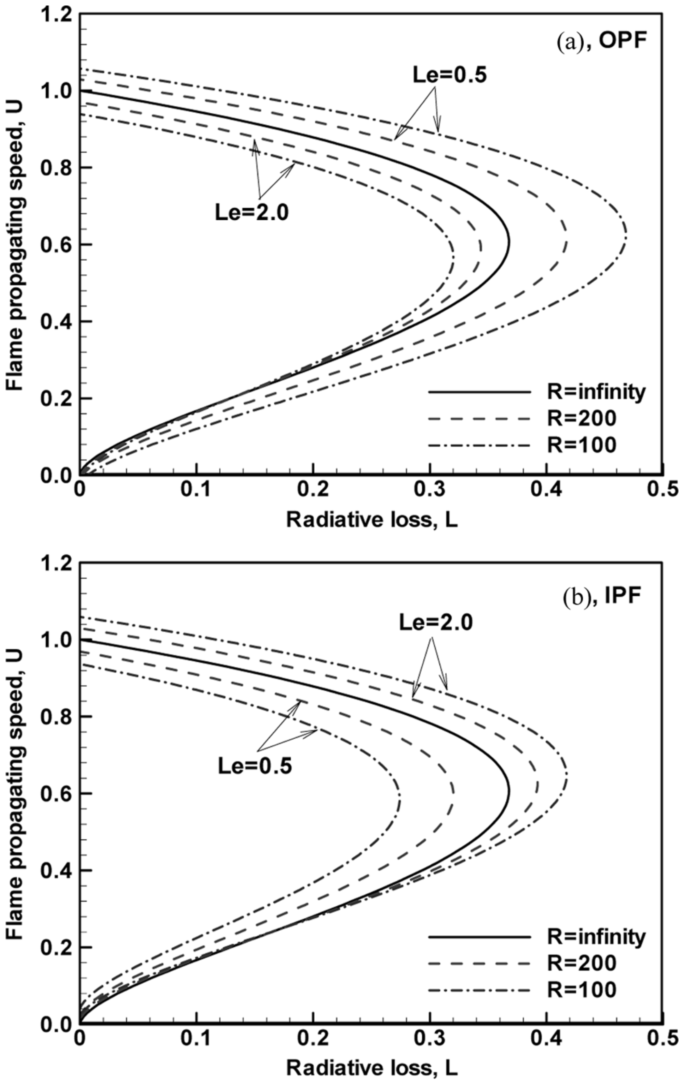

Figure 4 The flame propagating speed as a function of radiative loss for (a) OPF and (b) IPF at different flame radii and Lewis number.

always increases for $Le < 0.8$. For $0.8 < Le < 1.0$, the magnitude of the Markstein length can be smaller than the adiabatic Markstein length. For $Le > 1.0$, the normalized Markstein number is always greater than unity and increases with radiative loss. Due to the increase of Markstein number with radiation, both thermal-diffusion instability and pulsating instability can be enhanced by radiation.

In brief summary, the above theoretical analysis of OPF and IPF shows that flame propagation, flame extinction, and Markstein length are strongly affected by the Lewis number as well as radiative loss. For the method utilizing propagating spherical flames to measure laminar flame speed and Markstein length (Chen et al.,

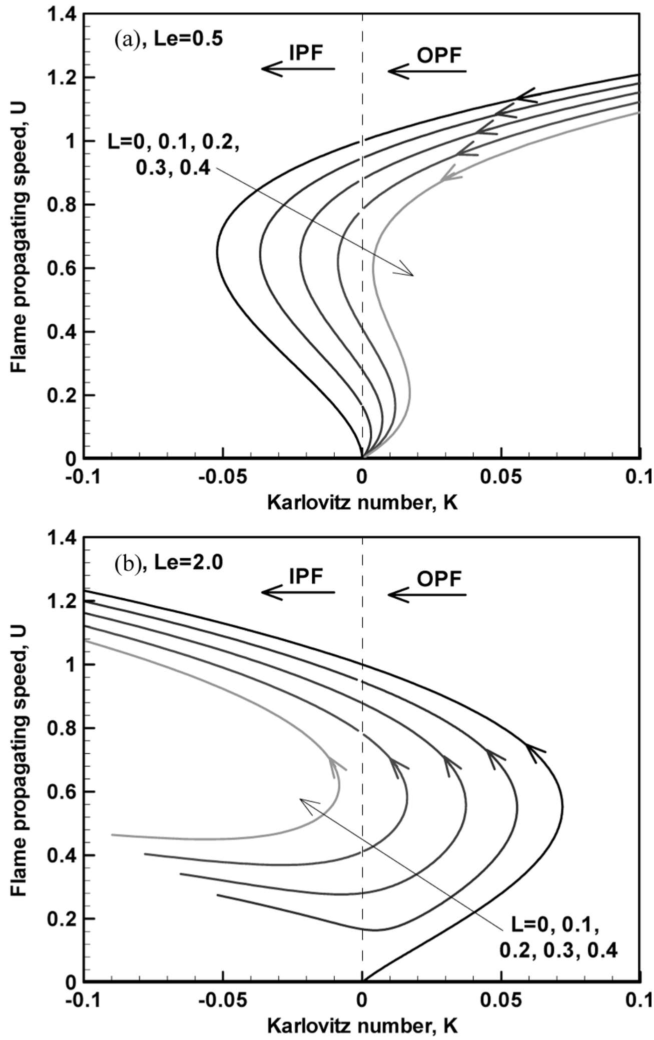

Figure 5 The flame propagating speed as a function of Karlovitz number for OPF and IPF with different radiative loss: (a) Le = 0.5; (b) Le = 2.0.

2009a, 2009b; and references therein), the effects of radiation depend on the magnitude of the normalized radiative loss intensity (L). For near-limit mixtures having very low laminar flame speed (less than 10 cm/s) and highly radiative mixtures (for example, CO_2-diluted mixtures in oxy-fuel combustion), we have $L > 0.1$ and thus the effect of radiation on the measured flame speed and Markstein length is not negligible. For most mixtures (H_2/air, CH_4/air, C_3H_8/air, etc.) not close to their flammability limits and without CO_2 dilution, we have $L < 0.05$ and the effects of radiation on flame speed and Markstein length can be neglected ($|U\text{-}1| < 5\%$ and $|Ma/Ma0\text{–}1| < 10\%$ for $L \leq 0.05$).

It is noted that the theory is based on the assumption of large flame radius and quasi-steadiness within the coordinate system attached to the flame. However, for

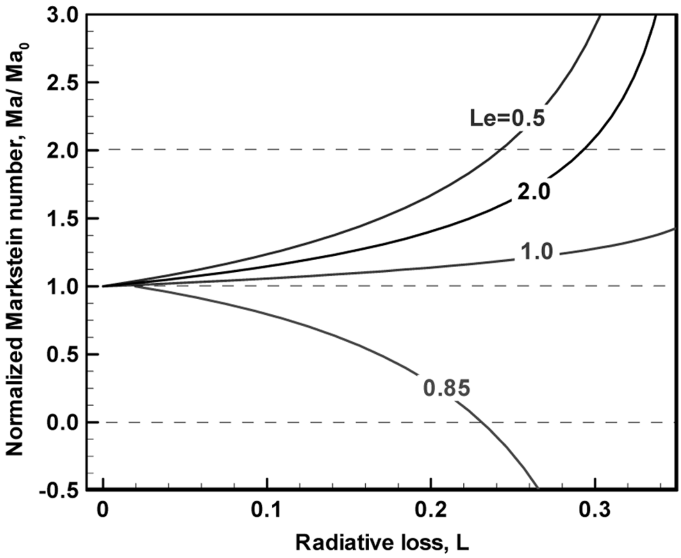

Figure 6 The normalized Markstein number as a function of radiative loss for different Lewis numbers.

IPF, extinction can take place at small flame radii, especially for small radiative loss (shown in Figure 3). As a result, an unsteady study, which is more naturally conducted in the laboratory frame, is required (Sun & Law, 1998). In the next section, unsteady simulations of OPF and IPF are conducted to validate the theoretical results, investigate the extinction of IPF, and examine whether there is unconsumed reactant for IPF with radiative loss.

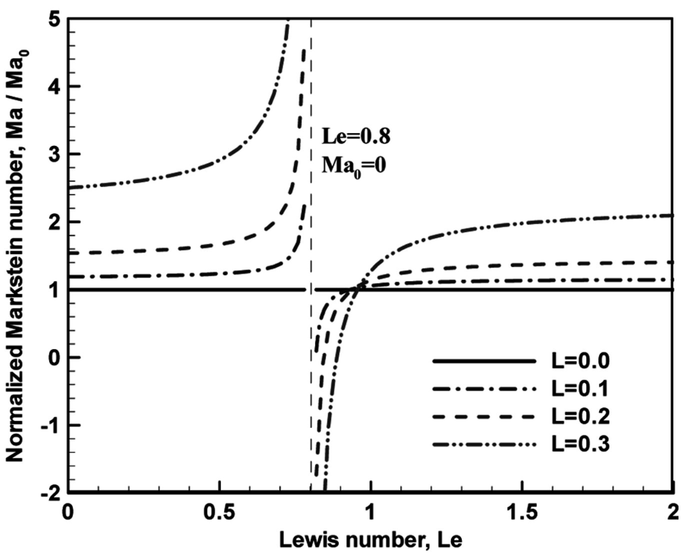

Figure 7 The normalized Markstein number as a function of Lewis number for different radiative loss.

NUMERICAL SIMULATION

Numerical Methods

The non-dimensional form of Eqs. (1) and (2) is solved numerically by means of an implicit finite volume method (Chen & Ju, 2007). To numerically resolve the moving flame front, a ten-level adaptive griding algorithm has been developed (Chen et al., 2007). The mesh addition and removal are based on the first- and second-order gradients of the temperature and reaction rate distributions. Uniform grids of 0.00125–0.01 (length normalized by flame thickness) are utilized to cover the reaction zone and are kept moving together with the flame front. The following finite reaction rate is used in the numerical simulation (Chen & Ju, 2007; Flaherty et al., 1985):

$$\omega = \frac{1}{2Le} \cdot Y \cdot Z^2 \cdot \exp\left[\frac{Z(T-1)}{\sigma + (1-\sigma)T}\right] \tag{25}$$

In all simulations, the computation domain length is 1000. The boundary conditions of zero gradient for temperature and fuel mass fraction are used at $r = 0$ and $r = 1000$. To initialize the flame, the flame ball solution (flame ball center at $r = 0$) is used as the initial condition for OPF, while the planar flame solution (flame front at $r = 1000$) is used for IPF.

Results and Discussions

Figure 8 shows the time evolution of reaction rate, fuel mass fraction, and temperature of IPF for $Le = 0.5$ with and without radiative loss. As expected by theoretical analysis, when the flame propagates inward, the burning intensity becomes progressively weaker due to the increase of the magnitude of flame stretch rate (negative for IPF) and $Le < 1$. When the radiative loss is not considered, Figure 8a shows that flame extinguishes around $R = 10$ instead of $R = 20$, as predicted by the theory in Figure 3a. This discrepancy is mainly due to the assumption of large flame radius and quasi-steadiness in theoretical analysis. When radiative loss is included, Figure 8b shows that flame extinguishes around $R = 56$, which is very close to $R = 54$ predicted by the theory shown in Figure 3a. Therefore, theoretical results for flames at large flame radii are consistent with prediction from numerical simulation.

Furthermore, Figure 8a shows that the extinction is induced by the complete depletion of fuel: at t_{20}, the fuel mass fraction is very close to zero throughout the computational domain, and the reaction rate is about three orders smaller than that of a planar flame (compared to that at t_0). From t_{20} to t_{25}, the temperature increase in the center is caused by thermal conduction, and there is slight decrease of the temperature in the region of $r > 23$ (which is not discernable in Figure 8a). This result is consistent with the simulation of lean hydrogen/air IPF conducted by Sun and Law (1998), who showed that all hydrogen is totally consumed by IPF.

Unlike the adiabatic case, when radiative loss is included, Figure 8b shows that there exists unconsumed reactant after extinction of IPF: at t_{18}, the reaction rate is very close to zero while the fuel mass fraction is larger than 0.1 for $r < 50$. After extinction, the fuel mass fraction in the center decreases due to mass diffusion.

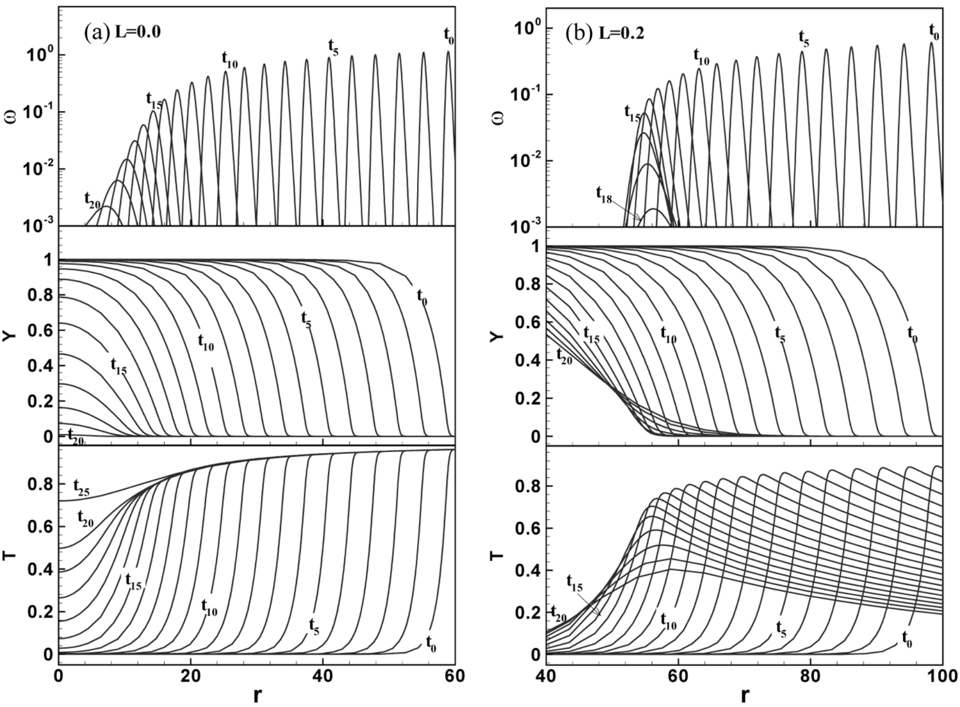

Figure 8 Time evolution ($t_i = t_0 + i\Delta t$) of different distributions of IPF for $Le = 0.5$: (a) $L = 0$; (b) $L = 0.2$.

The temperature in the center first increases and then decreases due to heat conduction and radiative loss. To further demonstrate the non-existence/existence of unconsumed reactant for IPF, we show the change of total amount of unburned fuel, $C = \int_0^\infty 4\pi r^2 Y(r)dr$, for IPF with different radiative loss intensities in Figure 9. It is seen that for adiabatic case ($L = 0$), C decreases to 0 when flame extinction occurs. Hence, there is no unconsumed reactant for adiabatic IPF. However, when radiation is considered, C is greater than 0 and remains to be constant after flame extinction occurs. Therefore, there is unconsumed reactant after extinction of IPF with radiative loss. As a result, for ultra-lean combustion in which radiative loss is not negligible, the unconsumed reactant in IPF will be a matter of concern: the extinction of IPF will be a source of unburned hydrocarbon and constitute a loss in the combustion efficiency. It is noted that the unconsumed reactant in IPF ($Le = 0.5$ and $L = 0.2$) is due to not only radiative loss but also negative flame stretch rate: when radiative loss is not considered, there is no unconsumed reactant for IPF; a planar flame without flame stretch can consume all the reactant in case of $Le = 0.5$ and $L = 0.2$.

Figure 10 shows the time evolution of reaction rate, fuel mass fraction, and temperature of IPF for $Le = 2.0$ with radiative loss. Unlike the case of $Le = 0.5$ and $L = 0.2$, Figure 10 shows that there is no unconsumed reactant left. This is because for mixture with Lewis number greater than unity, when the flame propagates inward, the burning intensity becomes progressively stronger due to the increase of the magnitude of flame stretch rate (negative for IPF). This observation

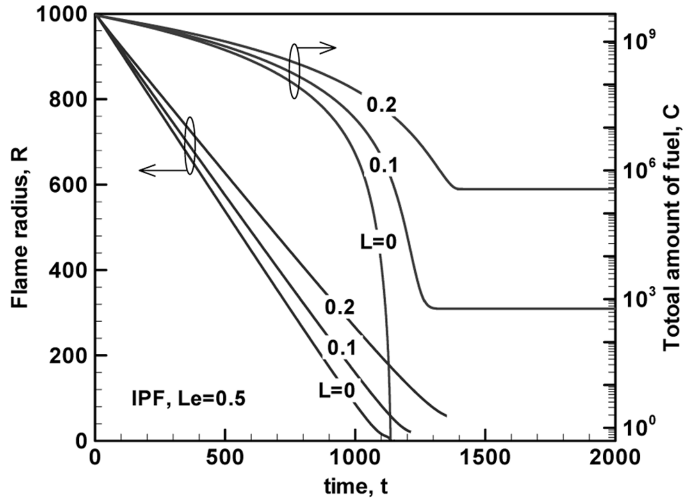

Figure 9 Change of the flame radius and the total amount of unburned fuel for IPF with different radiative loss.

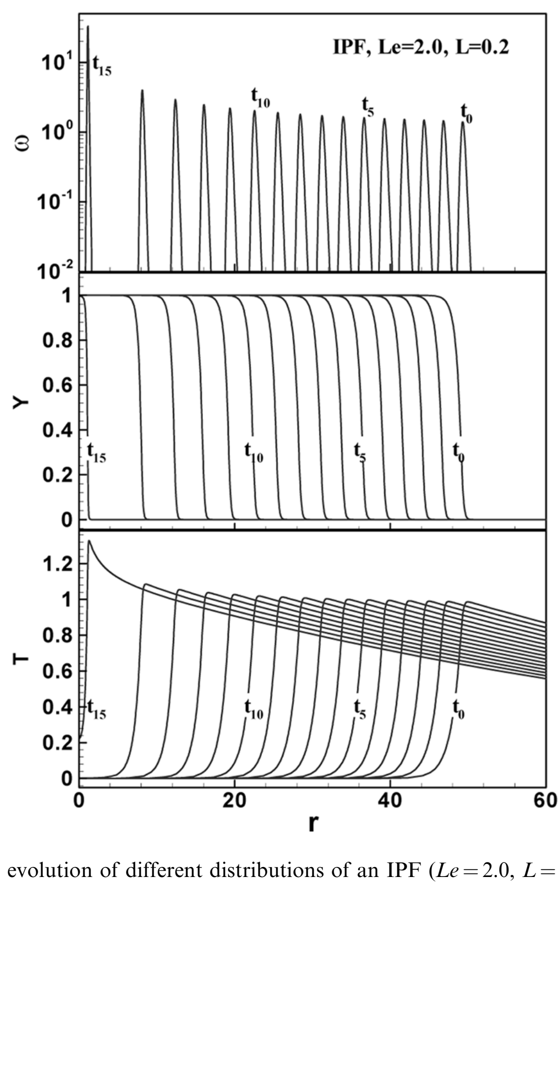

Figure 10 Time evolution of different distributions of an IPF ($Le = 2.0$, $L = 0.2$, $t_i = t_0 + i\Delta t$).

is consistent with theoretical results shown in Figure 3b. Therefore, for $Le > 1$, the IPF persists until the center, and hence all reactants are totally consumed even when radiative loss is considered. As such, unconsumed reactant in IPF for $Le > 1$ is expected not to be a matter of concern.

Simulations for OPF with different radiative loss and Lewis numbers are also conducted. All the results are summarized in Figure 11. Similar to theoretical results shown in Figure 3, numerical simulation also shows that the *U*-*R* diagram of OPF and IPF has totally opposite trends for $Le = 0.5$ and $Le = 2.0$: both OPF and IPF become progressively weaker during propagation for $Le = 0.5$ but become progressively stronger during propagation for $Le = 2.0$. Again, this is due to the combined effects of flame stretch and Lewis number. Figure 11 also shows that the flame propagation and extinction is strongly affected by radiative loss. Moreover, the Markstein length from numerical simulation is also found to increase with radiative loss for both $Le = 0.5$ and $Le = 2.0$, which is consistent with theory. It is noted that the flame propagating speed of a planar flame (at $R = 10^3$) for all Lewis numbers and radiative loss in Figure 11 is slightly lower than that in Figure 3. This is because the reaction rate is considered to be a Delta function (Eq. (10)) under the assumption of large activation energy assumption in theoretical analysis, while the finite reaction rate (Eq. (25)) is used in numerical simulation (Flaherty et al., 1985). Moreover, the initial transient ignition process affects the outwardly propagating flame speed for $R < 100$ (Chen et al., 2009b), which makes the flame speed predicted by numerical simulation (shown in Figure 11) slightly larger than that by theoretical analysis for OPF with $R < 100$ (shown in Figure 3).

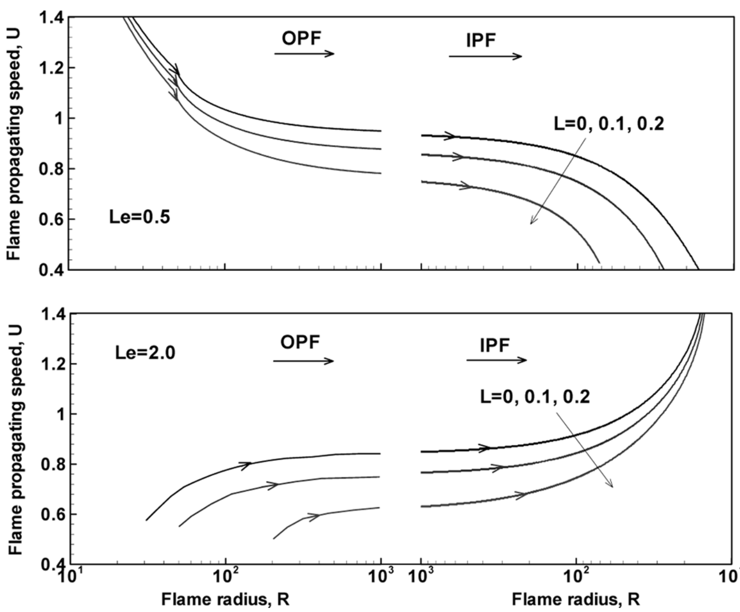

Figure 11 The flame propagating speed as a function of flame radius for OPF and IPF with different radiative loss and Lewis numbers (results from numerical simulation).

CONCLUSION

The OPF and IPF with radiative loss are studied using asymptotic analysis and numerical simulation. The theoretical analysis is based on the assumption of large flame radius and quasi-steadiness of flame propagation. A general correlation between flame propagating speed and flame radius for both OPF and IPF with radiative loss is derived and utilized to study the effects of radiative loss and Lewis number on flame propagation and extinction. It is shown that the flame propagating speed and flammability region are strongly affected by Lewis number as well as radiative loss. Opposite trends for the change of flame propagating speed during flame propagation are shown for OPF and IPF at different Lewis numbers. The positive/negative stretch rate of OPF/IPF is found to enhance/weaken the flame at a small Lewis number and to weaken/enhance the flame at a large Lewis number. As a result, the flammability region is correspondingly extended or reduced.

A correlation for Markstein length at different Lewis numbers and radiative loss is also derived from theoretical analysis. It is demonstrated that the Markstein length is strongly affected by radiative loss as well as Lewis number. Moreover, it is shown that for most mixtures not close to their flammability limits and without CO_2 dilution, the effect of radiation on the Markstein length measured from expanding spherical flames can be neglected, while the effect of radiation is not negligible for near-limit mixtures having very low laminar flame speed (less than 10 cm/s) and highly radiative mixtures (for example, CO_2-diluted mixture in oxy-fuel combustion).

To validate the theoretical results and determine whether there is unconsumed reactant for IPF, unsteady simulations are conducted. The results from numerical simulation agree qualitatively well with theoretical prediction for flames at large flame radii, which further shows the validity of theoretical analysis. Moreover, it is found that extinction of adiabatic IPF for $Le = 0.5$ is induced by the complete depletion of fuel, and there is no unconsumed reactant left. However, when radiative loss is considered, there exists unconsumed reactant after extinction of IPF for $Le = 0.5$. For a mixture of Lewis number larger than unity, the reactant is found to be totally consumed via IPF with/without radiative loss, as the burning intensity becomes progressively stronger due to the increase of the magnitude of flame stretch rate.

ACKNOWLEDGMENT

This work was partially supported by National Natural Science Foundation of China (Grant no. 50976003), State Key Laboratory for Turbulence and Complex Systems, and the U.S. Department of Energy. It is also a pleasure to acknowledge helpful discussions with Mr. Michael P. Burke at Princeton University.

REFERENCES

Bechtold, J.K., Cui, C., and Matalon, M. 2005. The role of radiative losses in self-extinguishing and self-wrinkling flames. *Proceedings of the Combustion Institute*, **30**, 177.

Buckmaster, J. 1976. Quenching of deflagration waves. *Combustion and Flame*, **26**(2), 151.

Buckmaster, J. 1997. The effects of radiation on stretched flames. *Combustion Theory and Modelling*, **1**(1), 1.

Buckmaster, J., and Lee, C.J. 1992. The effects of confinement and heat loss on outwardly propagating spherical flames. *Proceedings of the Combustion Institute*, **24**, 45.

Chen, Z., Burke, M.P., and Ju, Y. 2009a. Effects of compression and stretch on the determination of laminar flame speed using propagating spherical flames. *Combustion Theory and Modelling*, **13**(2), 343.

Chen, Z., Burke, M.P., and Ju, Y. 2009b. Effects of Lewis number and ignition energy on the determination of laminar flame speed using propagating spherical flames. *Proceedings of the Combustion Institute*, **32**, 1253.

Chen, Z., and Ju, Y. 2007. Theoretical analysis of the evolution from ignition kernel to flame ball and planar flame. *Combustion Theory and Modelling*, **11**(3), 427.

Chen, Z., and Ju, Y. 2008. Combined effects of curvature, radiation, and stretch on the extinction of premixed tubular flames. *International Journal of Heat and Mass Transfer*, **51**, 6118.

Chen, Z., Qin, X., Xu, B., Ju, Y., and Liu, F. 2007. Studies of radiation absorption on flame speed and flammability limit of CO_2 diluted methane flames at elevated pressures. *Proceedings of the Combustion Institute*, **31**, 2693.

Clavin, P. 1985. Dynamic behavior of premixed flame fronts in laminar and turbulent flows. *Progress in Energy and Combustion Science*, **11**(1), 1.

Flaherty, J.E., Frankel, M.L., Roytburd, V., and Sivashinsky, G.I. 1985. Numerical study of quenching of inward propagating spherical flames. *Combustion Science and Technology*, **43**(5–6), 245.

Frankel, M.L., and Sivashinsky, G.I. 1983. On effects due to thermal-expansion and Lewis number in spherical flame propagation. *Combustion Science and Technology*, **31**(3–4), 131.

Frankel, M.L., and Sivashinsky, G.I. 1984. On quenching of curved flames. *Combustion Science and Technology*, **40**, 257.

Huang, Z., Zhang, Y., Zeng, K., Liu, B., Wang, Q., and Jiang, D.M. 2006. Measurements of laminar burning velocities for natural gas-hydrogen-air mixtures. *Combustion and Flame*, **146**(1–2), 302.

Ishizuka, S. 1993. Characteristics of tubular flames. *Progress in Energy and Combustion Science*, **19**(3), 187.

Joulin, G., and Clavin, P. 1979. Linear-stability analysis of non-adiabatic flames: Diffusional-thermal model. *Combustion and Flame*, **35**(2), 139.

Ju, Y., Guo, H.S., Maruta, K., and Liu, F.S. 1997. On the extinction limit and flammability limit of non-adiabatic stretched methane-air premixed flames. *Journal of Fluid Mechanics*, **342**, 315.

Ju, Y., Matsumi, H., Takita, K., and Masuya, G. 1999. Combined effects of radiation, flame curvature, and stretch on the extinction and bifurcations of cylindrical CH_4/air premixed flame. *Combustion and Flame*, **116**(4), 580.

Law, C.K. 2006. *Combustion Physics*, Cambridge University Press, Cambridge, U.K.

Mitani, T. 1980. Asymptotic theory for extinction of curved flames with heat-loss. *Combustion Science and Technology*, **23**(3–4), 93.

Mosbacher, D.M., Wehrmeyer, J.A., Pitz, R.W., Sung, C.J., and Byrd, J.L. 2003. Experimental and numerical investigation of premixed tubular flames. *Proceedings of the Combustion Institute*, **29**, 1479.

Ronney, P.D., and Sivashinsky, G.I. 1989. A theoretical study of propagation and extinction of nonsteady spherical flame fronts. *SIAM Journal on Applied Mathematics*, **49**(4), 1029.

Sivashinsky, G.I. 1974. Converging spherical flame front. *International Journal of Heat and Mass Transfer*, **17**(12), 1499.

Sohrab, S.H., and Law, C.K. 1984. Extinction of premixed flames by stretch and radiative loss. *International Journal of Heat and Mass Transfer*, **27**(2), 291.

Spalding, D.B. 1957. A theory of inflammability limits and flame-quenching. *Proceedings of the Royal Society of London Series A: Mathematical and Physical Sciences*, **240**(1220), 83.

Sun, C.J., and Law, C.K. 1998. On the consumption of fuel pockets via inwardly propagating flames. *Proceedings of the Combustion Institute*, **27**, 963.

Taylor, S.C. 1991. Burning velocity and the influence of flame stretch. Ph.D. thesis, University of Leeds, Leeds, U.K.

Williams, F.A. 1985. *Combustion Theory*, Benjamin-Cummins, Menlo Park, Calif.